ISSN: 0975-8585

Research Journal of Pharmaceutical, Biological and Chemical Sciences

Hydrothermal synthesis of γ-MnO_2 star shape nanostructures and the effect of doping with (Fe and Cu) on their electrochemical performance in zinc-MnO_2 rechargeable batteries.

Zahraa Hasan Raheem[1]*, and Abdulkareem Mohammed Ali Alsammarraie[2].

[1]College of Agricultural Engineering Sciences, University of Baghdad, Iraq.
[2]College of Science, Department of chemistry, University of Baghdad, Iraq.

ABSTRACT

Star shaped γ-MnO_2 nanostructures have been successfully prepared by hydrothermal synthesis method using manganese sulphate monohydrate and sodium perchlorate at 160º C for 12 hours ,and then preparing doped samples of the same prepared star shaped γ-MnO_2 nanostructures with 5% of each of iron and copper separately for enhancing the electrochemical performance of these nanostructures. The chemical and structural characterization of the prepared materials were done using XRD, SEM, EDS, and Raman spectroscopy, and then the electrochemical performance of the assembled zinc-nanoMnO_2 rechargeable battery was done by electrochemical impedance spectroscopy (EIS) and galvanostatic charge – discharge, the results showed that the Cu doped sample had better electrochemical behavior , it had lower charge transfer impedance than the iron doped sample, and its specific capacity (306.8 mAh/g) and was very close to the theoretical specific capacity of MnO_2 .

Keywords: hydrothermal synthesis, manganese dioxide nanostructure, zinc-ion rechargeable battery.

Corresponding author

ISSN: 0975-8585

INTRODUCTION

In recent decades MnO_2 has been considered as a very promising metal oxide with potentials for different applications owing to its nontoxicity, natural abundance, high activity, and low cost compared with other transition metal oxides. It has been applied in different fields; biosensors [1-2], rechargeable batteries [3-7], supercapacitors [8-11], and catalysis [12-14]. MnO_2 has various polymorphs, such as α-, β-, γ- , δ- and λ [15,16] which differ in the way the basic units [MnO_6] octahedral are connected to each other in the crystal structure which gives raise to different tunnel size and shape for α (2x2),β(1x1), and γ(1x1 and 1x2) phases [17], and makes a layered structure in the case of δ-MnO_2. γ-MnO_2 has a complicated structure which can be considered as a random intergrowth of various amounts of pyrolusite phase (1x1) within a ramsdelite phase (1x2) as first described by De Wolff [18]. The tunnels inside the crystal structure have dimensions of (2.3Aº x2.3Aº) and (2.3Aº x4.6 Aº) for the (1x1) and (1x2) tunnels respectively [19, 20]. This crystal structure has been used for many years in secondary alkaline batteries and primary batteries. Although lithium ion batteries had taken over the rechargeable battery sales due to their high energy densities, however there are some concerns about these batteries; the high cost, limited sources of lithium, and because of using organic solvents that have explosive nature, which raised the need to develop other safer aqueous batteries [21]. Among the other available rechargeable batteries nowadays, rechargeable zinc – manganese dioxide aqueous batteries are considered the most convenient alternative [22]. The use of nanomaterials in batteries have improved their electrochemical performance [23] due to the small size of these materials which will lower the volume expansion during intercalation - deintercalation of cations from the electrolyte solution during repeated charge – discharge processes and will increase the contact surface area between the electrode / electrolyte and will decrease the length the diffusion path for both electrons and ions [24, 25].

Using mild aqueous electrolyte in these kind of batteries like zinc sulphate with a mild acidic pH (4-6) which showed some promising results [26, 27].

MATERIALS AND METHODS

All materials were used without further purification, $MnSO_4.H_2O$ (99%) supplied from Fluka, both Polyvinylidene difluoride (PVDF) (99%) and N-methyl-2- pyrrolidone (NMP) from Tob-new energy China, Sodium chlorate $NaClO_3$(99%) from BDH, copper nitrate tri hydrate Cu $(NO_3).3H_2O$ (99%) from Fluka, iron nitrate nona hydtrate $Fe(NO_3)_3.9H_2O$(98%) from Fluka, Zinc sulphate heptahydrate $ZnSO_4.7H_2O$ (99%) from Merk.

All the γ-MnO_2 nanostructures (undoped and doped with iron and copper) were prepared using hydrothermal synthesis method using a 100 ml Teflon liner placed into a stainless steel reactor , then the prepared materials were characterized using SHIMADZU (XRD) 6000 X-Ray diffractometter, Raman spectroscopy was performed using Senterra BRUKER, FE-SEM images to determine the morphology of the samples were done using FE-SEM Hitachi S-4160, and then these prepared samples were applied in aqueous zinc- ion rechargeable batteries, and was tested for electrochemical performance using Metrohm Autolab.

Experimental part

Materials synthesis

The undoped star shaped γ-MnO_2 nanostructures were synthesized by the reaction between $NaClO_3$ as an oxidizing agent and $MnSO_4.H_2O$ with mole ratio of (2:1). After taking weight of the starting materials they were dissolved in distilled water and magnetically stirred till the solution became clear, then transferred into 100 ml Teflon liner and hydrothermally treated at 160º C for 12 hours, after that it has been left to cool down naturally. Then the dark brown precipitate of γ -MnO_2 was collected and washed several times with distilled water and ethanol and then it was dried at 60ºC for overnight.

For the preparation of the doped samples, the same synthesis procedure of preparing undpoed γ-MnO_2 nano star shapes was used with the addition of (5 % weight) of $Fe(NO_3)_3.9H_2O$ into the reaction solution to prepare Fe doped γ- MnO_2 nano stars, and (5 % weight) $Cu(NO_3).3H_2O$ to prepare Cu doped γ- MnO_2 nano stars in two separate hydrothermal processes at 160ºC for 12 hours. Then the precipitate was collected, washed with distilled water and ethanol, and then dried at 60ºC for 12 hours.

Zinc-MnO_2 battery assembly:

The prepared undoped and doped MnO_2 samples were used to assemble a zinc/ MnO_2 battery, the MnO_2 cathode is prepared by mixing a ratio of 75:15:10 % of the prepared MnO_2 nanostructure powder, Polyvinylidene difluoride (PVDF) binder and carbon black respectively, the mixture was finely grinded with a mortar and then mixed with some drops of NMP solvent to make a past, this paste was applied on a titanium sheet as a current collector (with 1mm thickness) and dried in oven at 100ºC overnight. After that the battery was assembled by placing a layer of the cathode, a piece of filter paper soaked with $ZnSO_4$ (0.5M) electrolyte and the anode which is a zinc sheet (with 2mm thickness).

Characterization:

To determine the phase of the prepared nanostructures of γ-MnO_2 samples X-ray powder diffraction (XRD) patterns have been measured using Shimadzu (XRD 6000) x-ray diffractometer with Cu Kα radiation (λ=1.54056A°). The size and morphology have been examined using field emission scanning electron microscopy (FESEM Hitachi s-4160). Surface area of the prepared samples was done with N_2 adsorption at 77.35K using ThermoQuest SpA surface area analyzer. Electrochemical characterization galvanostatic charge-discharge, and electrochemical impedance spectroscopy were performed on the assembled batteries using Metrohm Autolab.

RESULTS AND DISCUSSION

XRD patterns of the prepared γ-MnO_2 nanostructures for the doped and undoped samples are shown in figure (1). All the diffraction peaks can be clearly indexed to pure phase of orthorhombic γ-MnO_2 and the peaks are with a good agreement with the standard reported data (JCPDS card No. 14-644, with lattice parameters a= 6.36Aº , b=10.15 Aº and c=4.09 Aº)**.**

Figure (2) shows the SEM images of the prepared γ-MnO_2 nanstars the morphology is six branched crystal or a star like shape with dimensions of ~140 nm near the center of the star shape and around 55-70nm near the tips, and with variable lengths about 1.5-8 µm.

The EDS analysis for doped γ-MnO_2 nanostars in figures (4) and (5) showed that the doping percent practically is about 5% Fe and 3% for Cu indicating the successful doping process for these nanostructures especially in the case of Fe doped sample.

Raman scattering spectra shown in Fig (6) for the prepared pure and the doped γ -MnO_2 nano stars samples it clearly shows that the samples have the same pattern, the peaks in the region between (500-700 cm^{-1}) are characteristic for γ -MnO_2 [28], the two sharp peaks at 582 and 658cm^{-1} are attributed to stretching mode of Mn-O bond in the [MnO_6] octahedral units [29].

The BET analysis for the undoped prepared sample showed specific surface area of (9.16 m^2/g), the low surface area is may be due to the agglomeration of these structures as shown in the SEM images in figure (2).

For the estimation of the electrochemical behavior of the prepared samples, electrochemical analysis including charge-discharge analysis and electrochemical impedance spectroscopy (EIS) were used to test the undoped and doped samples. The practical specific capacity was calculated from the results of the charge-discharge according to the following equation [30]:

$$C_s = \frac{\mathrm{i\,x\,t}}{\mathrm{m}} \qquad \text{eq.1}$$

Where i is the applied current, t is the discharge time and m is the weight of the active material. And the calculated values of the specific capacities are listed in table (1). The highest value for the specific capacity of the prepared samples was for the Cu doped γ-MnO_2 nano star shape, this value is very close to the theoretical specific capacity of MnO_2 (308.3 mAh/g). The Nyquist plots in figure (10) showed a small semicircle and a straight line for the three samples, and figure (11) shows the equivalent circuit diagram for fitting the EIS

ISSN: 0975-8585

data. In this diagram, the equivalent circuit consist of R1 which represents the ohmic resistance of the solution, R2 is the interface resistance ,R3 represent the charge transfer resistance , QEP represents a constant phase element which represents the double layer capacitance and W is Warburg diffusion impedance which is related to the diffusion of Zn^{+2} ions in the lattice of MnO_2 , (R2/QEP1) represents impedance of the interphase between the electrolyte and the surface layer of MnO_2 that is in contact with the electrolyte solution, and (R3/QEP2) represents the charge transfer resistance. The EIS results in table (1) showed the lowest charge transfer impedance for the Cu doped sample then for the Fe doped sample and then for the undoped sample, the Cu doped sample showed the smallest semicircle indicating that the Cu doped sample has the better capacitance behavior and the sharp line which is attributed to the low charge transfer impedance and better diffusion process, these results are may be due the fact that the copper has higher conductivity than the other elements, also the lower oxidation state of the dopants lead to having more negative charges and this will lead to the increase of the cations like (K^+) inside the crystal tunnels to balance the total charge , which can improve the conductivity throw having oxygen vacancies[31, 32].

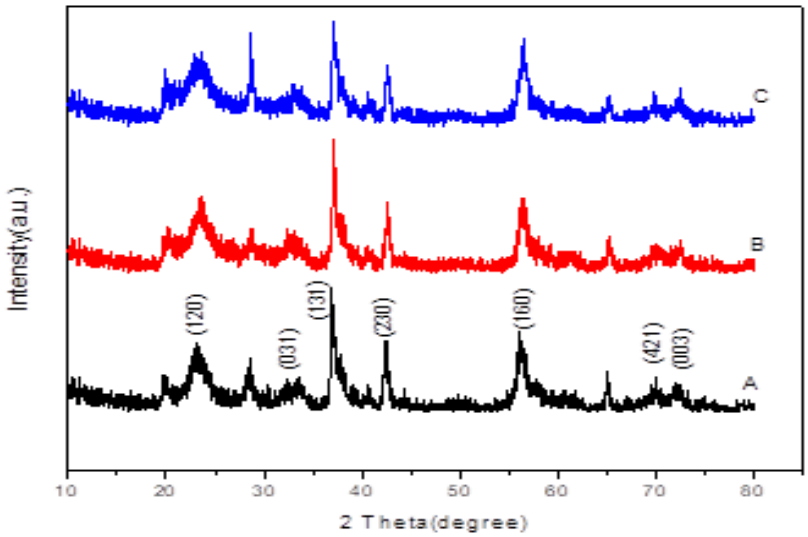

Figure 1: XRD patters for (A) undoped γ-MnO_2 nanstars, (B) 5% Cu doped γ-MnO_2 nanstars and (C) 5% Fe doped γ-MnO_2 nanstars.

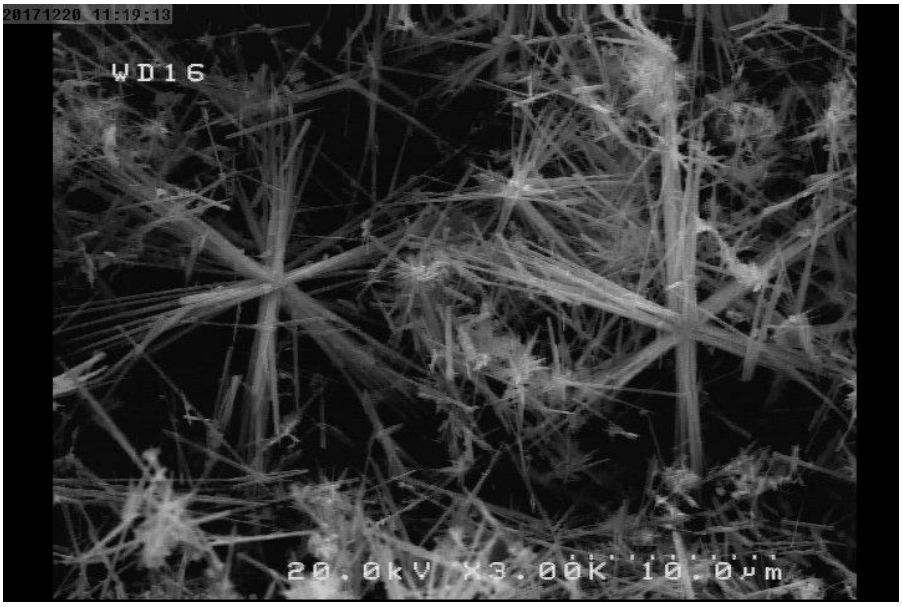

ISSN: 0975-8585

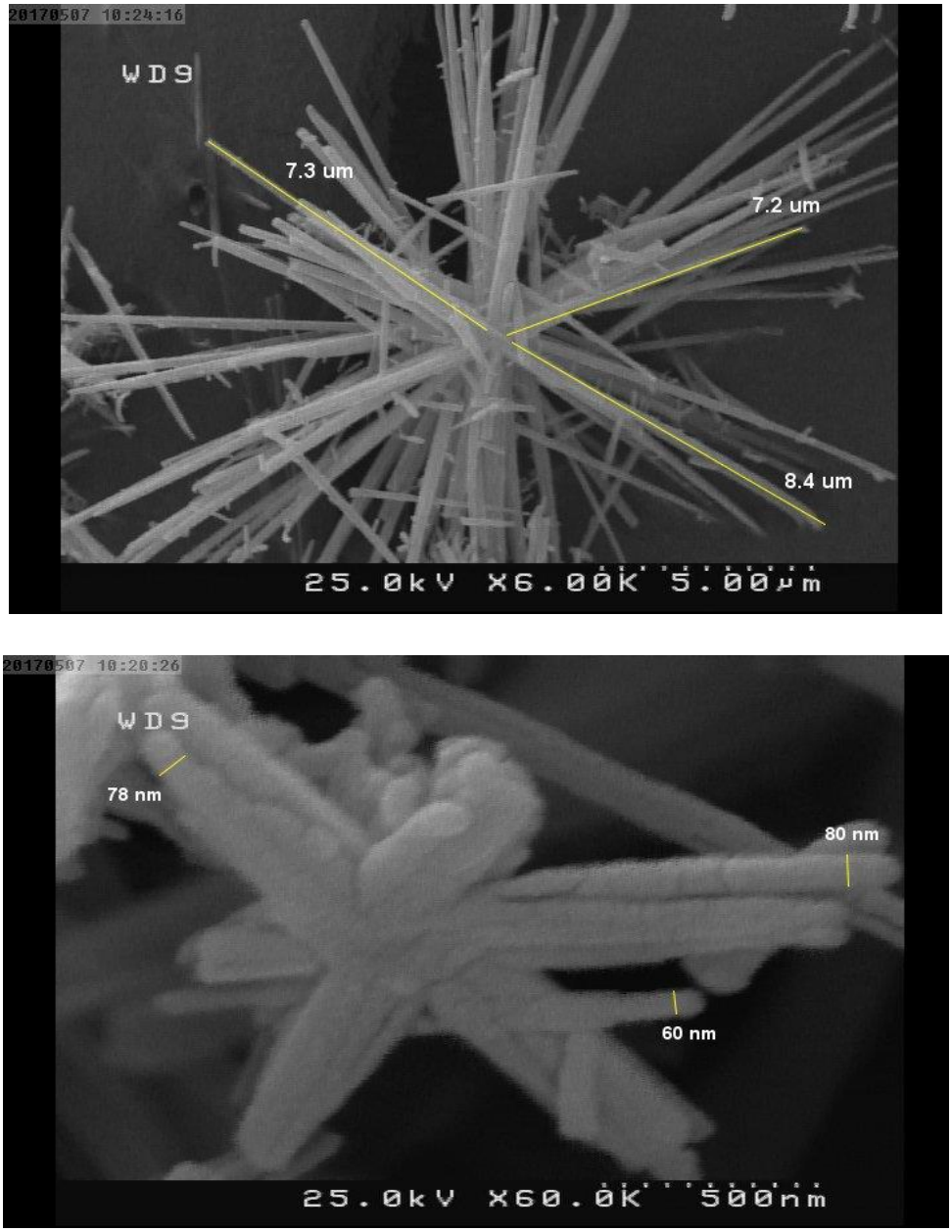

Figure 2: FE-SEM images of the prepared star like γ-MnO_2 nanostructure in different magnifications.

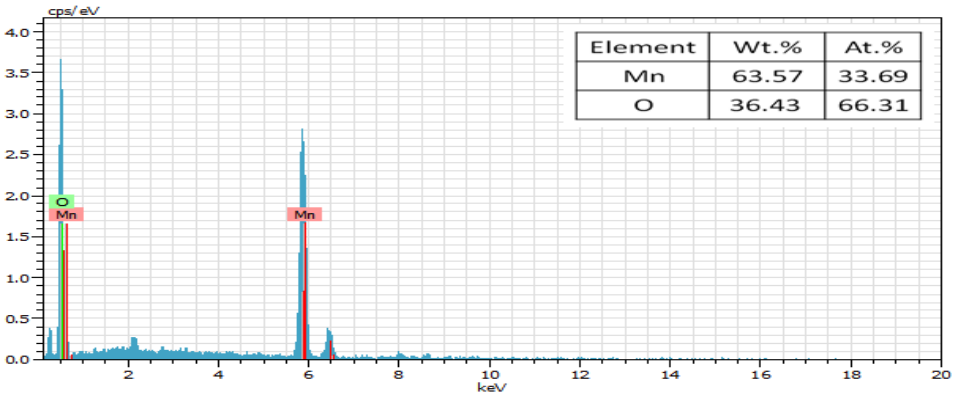

Figure 3: The EDS analysis for undoped γ-MnO_2 nanostars with table showing the weight and atomic percent of the detected elements.

ISSN: 0975-8585

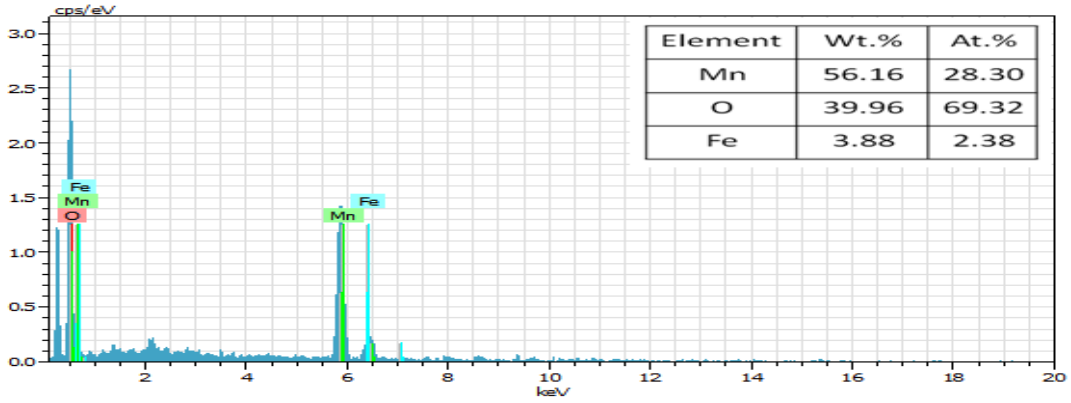

Figure 4: The EDS analysis for γ-MnO_2 nanostars doped with 5% Fe with table showing the weight and atomic percent of the detected elements.

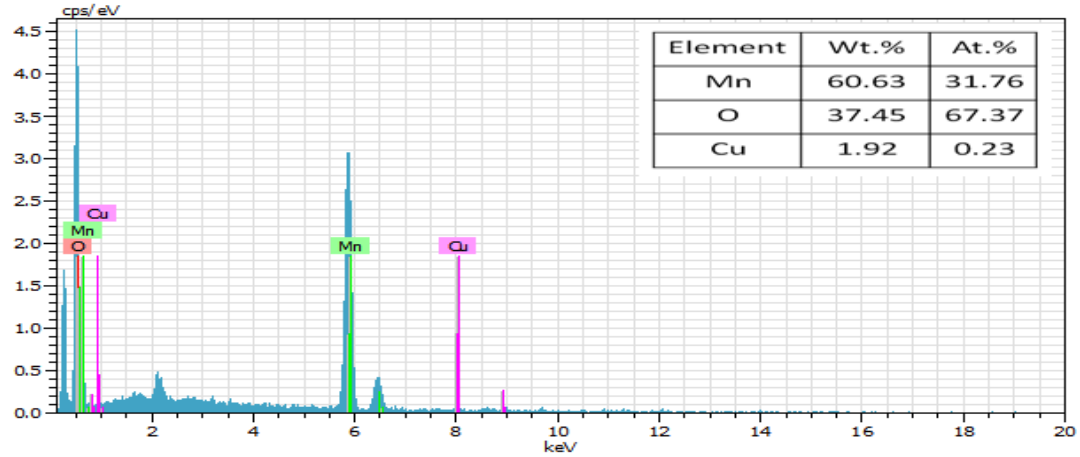

Figure 5: The EDS analysis for γ-MnO_2 nanostars doped with 5% Cu with table showing the weight and atomic percent of the detected elements.

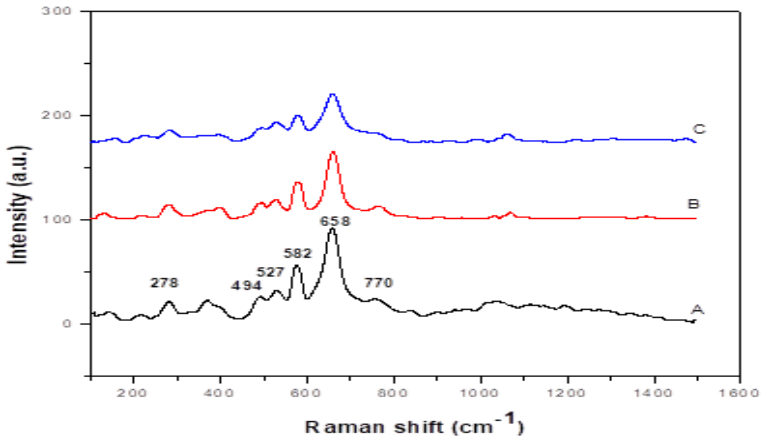

Figure 6: Raman scattering spectra for (A) undoped γ-MnO_2 nanostars (B) γ-MnO_2 nanostars doped with 5% Cu (C) γ-MnO_2 nanostars doped with 5% Fe.

ISSN: 0975-8585

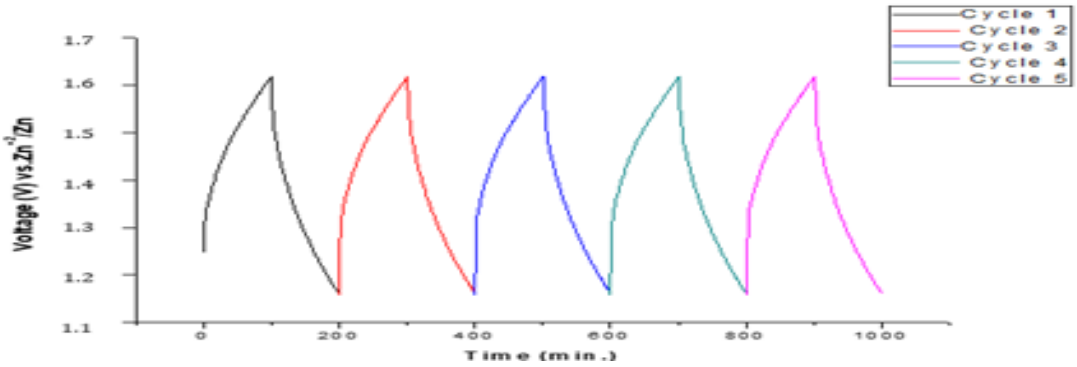

Figure 7: Charge and discharge plot for γ- MnO_2 nanostars.

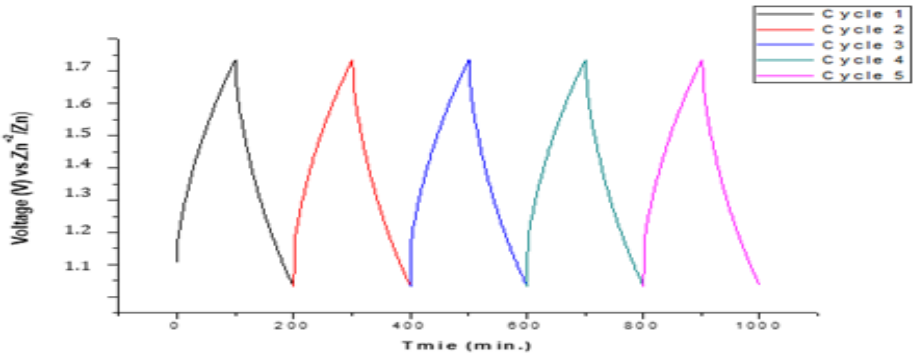

Figure 8: Charge and discharge plot for γ- MnO_2 nanostars doped with 5% Fe.

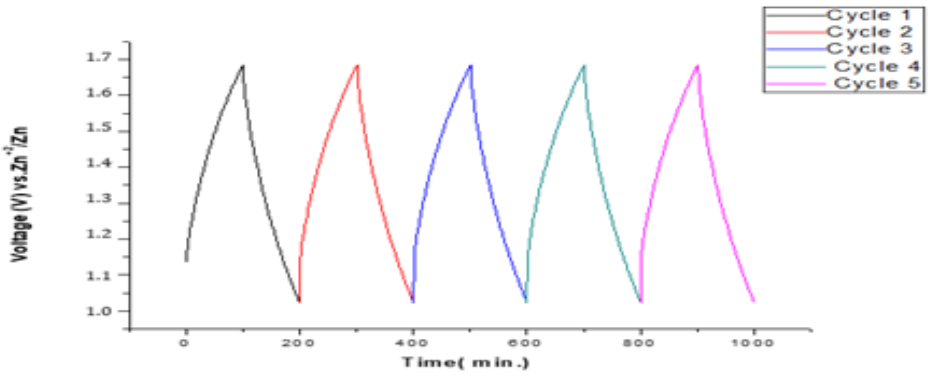

Figure 9: Charge and discharge plot for γ- MnO_2 nanostars doped with 5% Cu.

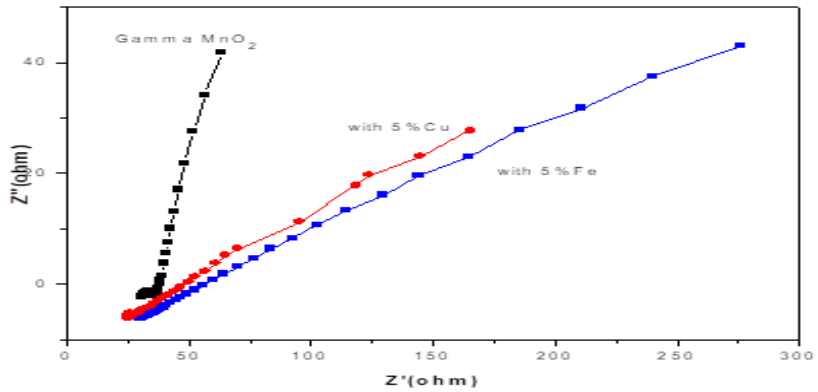

Figure 10: Nyquist plots for undoped γ-MnO_2 nanostars (in black), γ- MnO_2 nanostars doped with 5% Cu (in red color) and γ- MnO_2 nanostars doped with 5% Fe (in blue)

ISSN: 0975-8585

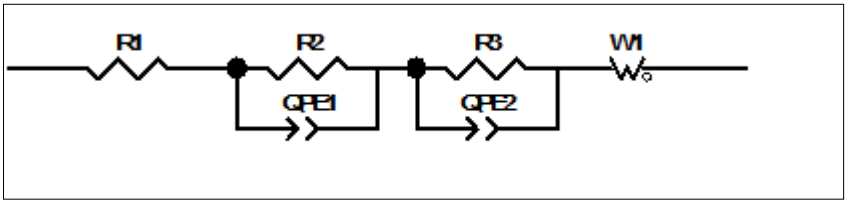

Figure 11: Diagram of equivalent circuits to fit the EIS data.

Table (1): The electrochemical parameters for the prepared undoped γ-MnO_2 nanostars and doped with 5% Fe and 5% Cu.

Sample name	R_s value (ohm)	R_{ct} value (ohm)	Specific capacity (mAh/g)
Undoped γ-MnO_2 nanostars	29.28	5.59	203.53
γ-MnO_2 nanostars doped with 5% Cu	24.87	3.17	306.8
γ-MnO_2 nanostars doped with 5% Fe	26.113	3.59	290.5

CONCLUSIONS

γ-MnO_2 star shape nanostructures and 5% Fe and 5%Cu doped γ-MnO_2 nanostars have been successfully prepared by a one step hydrothermal synthesis method. These nanostructures were applied in zinc-ion rechargeable battery with mild electrolyte using aqueous solution of zinc sulphate (0.5 M) for studying the effect of doping with some transition metals on the electrochemical behavior of these nanostructures. The calculated specific capacity of Cu-doped sample was higher than the other samples and was very close to the theoretical value of the specific capacity of the MnO_2 and the Fe doped sample also showed higher specific capacity than the undoped sample, and the EIS data showed that the Cu-doped sample has lower charge transfer impedance, which indicates that doping MnO_2 with these transition metals give an enhancement for the electrochemical properties of MnO_2 cathode.

ACKNOWLEDGEMENT

I would like to express my sincere thanks and gratitude to the staff of X-ray lab unit at the central lab in college of Ibn Al Haitham -Baghdad University for all their help. And many thanks to the staff of the central lab in chemistry department at college of science – Baghdad University for their help.

REFERENCES

[1] Bai YH, Du Y, Xu JJ, Chen HY. Electrochemistry Communications 2007; 9(10): 2611-2616.
[2] Liu Y, Zhang X, He D, Ma F, Fu Q, Hu Y. RSC Advances 2016;6(22): 18654-18661.
[3] Zhao J, Tao Z, Liang J, Chen J. Crystal Growth and Design 2008; 8(8): 2799-2805.
[4] Truong TT, Liu Y, Ren Y, Trahey L, Sun Y. ACS nano 2012; 6(9): 8067-8077.
[5] Pan H, Shao Y, Yan P, Cheng Y, Han KS, Nie Z, Mueller KT. Nature Energy 2016; 1(5):16039.
[6] Wruck WJ, Reichman B, Bullock KR, Kao WH. Journal of The Electrochemical Society 1991; 138(12): 3560-3567
[7] Su D, Ahn HJ, Wang G. NPG Asia Materials 2013; 1(15): 4845-4850.
[8] Wei C, Pang H, Zhang B, Lu Q, Liang S, Gao F. Scientific reports 2013; 3: 2193.
[9] Yang Y, Liu T, Zhang L, Zhao S, Zeng W, Hussain S, Peng X. Materials in Electronics 2016; 27(6): 6202-6207.
[10] Wang JW, Chen Y, Chen B Z. Metals and Materials International 2014; 20(6): 989-996.
[11] Jia Z, Wang J, Wang Y, Li B, Wang B, Qi T, Wang X. Journal of Materials Science & Technology 2016; 32(2): 147-152.

[12] Zhang J, Li Y, Wang L, Zhang C, He H. Catalysis Science & Technology 2015; 5(4): 2305-2313.
[13] Cheng F, Su Y, Liang J, Tao Z, Che J. Chemistry of Materials 2009; 22(3): 898-905.
[14] Roche I, Chaînet E, Chatenet M, Vondrák J. The Journal of Physical Chemistry C 2007; 111(3):1434-1443.
[15] Post JE. Proceedings of the National Academy of Sciences, 1999; 96(7):3447-3454.
[16] Thackeray MM. Progress in Solid State Chemistry 1997; 25(1-2):1-71.
[17] Wei W, Cui X, Chen W, Ivey DG.. Chemical society reviews 2011; 40(3): 1697-1721.
[18] De Wolff PM. Acta Crystallographica 1959; 12(4): 341-345.
[19] Ji C, Ren H, Yang S. RSC Advances 2015; 5(28): 21978-21987.
[20] Zhang Y, Sun C, Lu P, Li K, Song S, Xue D. CrystEngComm 2012; 14(18): 5892-5897.
[21] Kordesh K, Weissenbacher M. Journal of power sources 1994; 51(1-2): 61-78.
[22] Stani A, Taucher-Mautner W, Kordesch K, Daniel-Ivad J. Journal of power sources 2006; 153(2): 405-412.
[23] Poizot P, Laruelle S, Grugeon S, Dupont L, Tarascon M. Nature 2000; 407(6803): 496.
[24] Jin Y, Chen H, Chen M, Liu N, Li Q. ACS applied materials & interfaces 2013; 5(8): 3408-3416.
[25] Vu A, Qian Y, Stein A. Advanced Energy Materials 2012; 2(9): 1056-1085.
[26] Shoji T, Hishinuma M, Yamamoto T. Journal of applied electrochemistry 1988; 18(4): 521-526.
[27] Sun W, Wang F, Hou S, Yang C, Fan X, Ma Z, Wang C. Journal of the American Chemical Society 2017; 139(29): 9775-9778.
[28] Sun M., Lan B, Lin T, Cheng G, Ye F, Yu L, Zheng X. CrystEngComm, 2013; 15(35): 7010-7018.
[29] Julien C, Massot M, Rangan S, Lemal M, Guyomard D. Journal of Raman Spectroscopy 2002; 33(4): 223-228.
[30] Xu C, Chen Y, Shi S, Li J, Kang F, Su D. Scientific reports, 2015; 5: 14120.
[31] Davis DJ, Lambert TN, Vigil JA, Rodriguez MA, Brumbach MT, Coker EN, Limmer SJ.. The Journal of Physical Chemistry C 2014; 118(31): 17342-17350.
[32] Lo VC, Chung WW, Cao H, Dai X. (). Investigating the effect of oxygen vacancy on the dielectric and electromechanical properties in ferroelectric ceramics. Journal of applied physics 2008; 104(6): 064105.